J Ind Microbiol Biotechnol (2011) 38:1345–1357
DOI 10.1007/s10295-010-0918-z

ORIGINAL PAPER

Phenotypic characterization of *Corynebacterium glutamicum* under osmotic stress conditions using elementary mode analysis

Meghna Rajvanshi · K. V. Venkatesh

Received: 24 August 2010 / Accepted: 18 November 2010 / Published online: 5 December 2010

Abstract *Corynebacterium glutamicum*, a soil bacterium, is used to produce amino acids such as lysine and glutamate. *C. glutamicum* is often exposed to osmolality changes in its medium, and the bacterium has therefore evolved several adaptive response mechanisms to overcome them. In this study we quantify the metabolic response of *C. glutamicum* under osmotic stress using elementary mode analysis (EMA). Further, we obtain the optimal phenotypic space for the synthesis of lysine and formation of biomass. The analysis demonstrated that with increasing osmotic stress, the flux towards trehalose formation and energy-generating pathways increased, while the flux of anabolic reactions diminished. Nodal analysis indicated that glucose-6-phosphate, phosphoenol pyruvate, and pyruvate nodes were capable of adapting to osmotic stress, whereas the oxaloacetic acid node was relatively unresponsive. Fewer elementary modes were active under stress indicating the rigid behavior of the metabolism in response to high osmolality. Optimal phenotypic space analysis revealed that under normal conditions the organism optimized growth during the initial log phase and lysine and trehalose formation during the stationary phase. However, under osmotic stress, the analysis demonstrated that the organism operates under suboptimal conditions for growth, and lysine and trehalose formation.

Keywords *Corynebacterium glutamicum* · Osmotic stress · Elementary mode analysis · Nodal analysis · Flux analysis

Introduction

Corynebacterium glutamicum is a gram-positive, non-pathogenic soil bacterium, which is of immense industrial importance due to its ability to produce lysine and glutamate on a large scale. Osmotic stress is a major stress factor encountered by this bacterium both in its natural habitat and during industrial fermentation. Being a soil bacterium, hyper- and hypoosmotic stress conditions occur during periods of drought and the rainy season, respectively, in its natural habitat. During industrial fermentation for amino acid production, the organism experiences osmotic stress caused by either high substrate or product concentration. The study of osmotic stress is therefore of vital importance as it significantly affects growth behavior and production of primary and secondary metabolites by microorganisms [32]. Studying the adaptive behavior of *C. glutamicum* under stress is also helpful in understanding the survival strategies of pathogenic organisms like *Mycobacterium tuberculosis*, which belongs to the same suborder (*Corynebacterineae*) as that of the *C. glutamicum* [24, 29]. Because of frequent encounters with fluctuations in the osmolality, *C. glutamicum* has developed efficient methods to cope with the conditions of hypo- and hyperosmotic stress. In this study, we primarily focus on the adaptability of *C. glutamicum* to hyperosmotic stress conditions and analyze the adaptability of its metabolic network under such conditions.

Electronic supplementary material The online version of this article (doi:10.1007/s10295-010-0918-z) contains supplementary material, which is available to authorized users.

M. Rajvanshi
Department of Biosciences and Bioengineering, Indian Institute of Technology, Bombay, Powai, Mumbai 400076, India

K. V. Venkatesh (✉)
Department of Chemical Engineering, Indian Institute of Technology, Bombay, Powai, Mumbai 400076, India
e-mail: venks@iitb.ac.in

Hyperosmotic stress is a situation when the solute concentration in the interior of the cell is lower than that of its environment. The instant response to hyperosmotic shock is efflux of water from the cell. However, in some gram-positive strains like *Bacillus*, *Staphylococcus aureus* [14], and *C. glutamicum* [27], and gram-negative strains like *Azotobacter vinelandii* [12], both cell and cytoplasmic volume decrease spontaneously and no plasmolysis is observed. Cell dehydration due to hyperosmotic stress leads to growth inhibition, because dehydration along with reduced cell volume leads to increased concentration of all the intracellular metabolites, thus resulting in a reduced water activity—the normal range of which is essential for functioning of biological macromolecules. This results in inhibition of cellular processes like uptake of nutrients, DNA replication, etc., thereby leading to impaired cell growth [4].

The cell overcomes this hyperosmotic state by increasing the concentration of certain solutes either by uptake or synthesis [34]. This reduces water activity without increasing the concentration of all cytoplasmic components to toxic levels. Cell volume and turgor pressure also get restored to their prestress levels. Because this metabolic response of accumulation of osmoregulators is slow, it cannot prevent the initial volume reduction [27]. Osmoregulators which get accumulated in the cell in response to hyperosmotic shock are termed compatible solutes because they do not inhibit the vital cellular processes greatly. Compatible solutes have two fundamental properties. Firstly, they rehydrate the cell, thus restoring the growth by increasing osmolarity inside the cell, as compatible solutes can accumulate up to molar levels without interfering with the cellular functions [11]. Secondly, they stabilize the native structure of proteins by allowing their preferential hydration [1, 11].

The prominent compatible solutes found in bacteria are K^+, amino acids (e.g., glutamate, proline, and glutamine), quaternary amines (glycine betaine, carnitine), sugars (sucrose and trehalose), and tetrahydropyrimidines (ectoine) [13, 22]. Good osmoregulators are uncharged or zwitterionic organic solutes that have low molecular mass and are highly soluble in the cytoplasm [28]. Morbach and Kramer [18] reported that *C. glutamicum* prefers uptake of compatible solutes over their de novo synthesis because of the low energy cost. In several bacteria, like *Escherichia coli* or *Bacillus subtilis*, the immediate response to hyperosmotic shock with NaCl is fast uptake of K^+ [34]. This is the first step in the rehydration of the cell, as it increases the internal osmolarity. In *C. glutamicum* ambiguity prevails with respect to this immediate response. Guillouet and Engasser [9] reported accumulation of Na^+ upon sudden osmotic up-shock with NaCl, whereas Morbach and Kramer [19] reported significant increase in the concentration of internal K^+ from 450 to 800 μmol/g cell dry weight (CDW) upon increase in osmolality from 0.9 to 2.4 osmol/kg. To maintain electroneutrality, the accumulation of K^+ is accompanied by increase in the glutamate pool (major anionic organic solute [5]) by de novo synthesis [10]. This rapid accumulation of glutamate leads to temporary increase in the concentration of glutamine, as glutamine is generated from glutamate through a single reaction step. However, K^+, glutamate, and glutamine are not good osmoregulators because of their charge, low solubility, and free amino groups in the case of glutamate and glutamine. Therefore, in the second phase of osmotic response, ions are exchanged by neutral solutes like proline, trehalose, etc. [5, 28]. At low osmolalities (0.4 osmol/kg), trehalose and glutamate are the main compatible solutes but at higher osmolalities proline plays a dominant role [9]. Skjerdal et al. [28] reported that at higher osmolalities the concentrations of glutamine and glutamate are highest immediately after shock; the concentration of trehalose also increases as compared with the unstressed state. But as time progresses the concentration of proline increases, which represents at least 25% of the total intracellular osmolytes. Increased contribution of proline indicates that it is a more potent alleviator of stress. Ronsch et al. [25] observed that in the stationary phase proline concentration drops to a very low level, which shows that *C. glutamicum* does not actively regulate its solute pool to counteract hyperosmotic stress in the stationary phase. The concentration of glutamate neither changes with the course of fermentation nor with increased osmolality. This shows that glutamate does not have importance in the long-term adaptation but may be important in osmotic response after sudden increase in the external osmolality. The concentration of internal trehalose increases from an undetectable level during the course of fermentation and reaches a maximum (200 mM) in the stationary phase. This indicates that trehalose is also an important component for long-term adaptation and is the main protecting agent in the stationary phase [25]. Extracellular concentration of trehalose increases with increasing osmolality of the medium [7, 25].

A two-component system MtrAB is responsible for osmosensing and osmosignaling in *C. glutamicum* in response to hyperosmotic stress [15]. MtrB gets stimulated by high concentration of K^+, various solutes, sugar, amino acids, and polyethylene glycol [16, 17]. MtrAB regulates expression of genes involved in cell wall biosynthesis and genes of three transporters (BetP, ProP, and LcoP), which accumulate compatible solutes inside the cell [2, 15]; however, upregulation of osmolyte carrier ProP was highest among all proteins [2].

Studies described so far have concentrated on the physiological behavior of *C. glutamicum* under osmotic stress conditions. Varela et al. [32] for the first time

quantified metabolic response in terms of metabolic flux redistribution in *C. glutamicum* grown under discrete and gradient continuous culture to gradually increasing osmolarity (between 270 and 1,880 mosmol/kg). Varela et al. [33] also estimated the alteration in the maintenance coefficients of substrate and ATP under osmotic stress conditions using flux balance analysis. In the current study, we aim to quantify the metabolic fluxes across the network using the elementary mode approach. Elementary mode analysis (EMA) is a network-based pathway analysis method [21]. The advantage offered by EMA in comparison to other individual reaction-based approaches such as flux balance analysis (FBA) is that it links all the metabolites involved in the pathway from substrates to products. Thus each elementary mode takes into account the combined effect of all the individual reactions that participate in the entire pathway. This approach of flux analysis therefore becomes more systemic in nature as it depicts a more realistic picture of the functioning of the network [21, 26, 30]. Although Gayen and Venkatesh [7] evaluated the fluxes of elementary modes and characterized optimal phenotypic space using elementary modes for *C. glutamicum*, they did not examine metabolism under osmotic stress conditions. The present work intends to fill this gap, where optimal phenotypic space for biomass, trehalose, and lysine is obtained by using the stoichiometry of the set of elementary modes. Such an analysis is important, as characterization of the phenotypic space of an organism offers insight into the stoichiometric limits of uptake rates of oxygen and ammonia to produce various metabolites under stress. This study should help in understanding the phenotypic capability of *C. glutamicum* under osmotic stress.

Methodology

Strain and culture conditions

Corynebacterium glutamicum CECT 79 was obtained from Spanish Type Culture Collection, Valencia, Spain, and was used for all the experiments conducted. This strain requires biotin, homoserine (threonine and metheonine), and leucine for growth and produces lysine under threonine limitation conditions. Seed culture was prepared in LB5G broth by inoculating a loopful of culture in the medium contained in a triple-baffled flask. Culture was grown overnight in a rotatory shaker at 150 rpm and 30°C. 10% (v/v) culture was then transferred to preculturing medium and grown for 7–8 h maintaining the same rpm and temperature. Fermentation medium containing 100 g/l glucose was then inoculated with 10% (v/v) preculture seed. Details of the composition of seed, preculture, and fermentation media were reported previously [31]. pH of the media was adjusted to 7. Fermentation was performed in a laboratory bioreactor (BIOSTAT® B+ (Sartorius BBI Systems, Schwarzenberger, Melsungen, Germany)) with 1.5-l working volume. A constant airflow of 1.0 VVM (volume of air per volume of media per minute) was maintained throughout the fermentation. Stirrer speed was maintained at 1,000 rpm and temperature was kept at 30°C. pH was maintained at 7 by feeding 2.5 N NaOH via a peristaltic pump. Osmotic stress was created by adding NaCl into the media. Two concentrations of NaCl viz. 25 and 40 g/l were used to analyze the effect of low and high osmotic stress condition on the phenotypic state of *C. glutamicum* and were compared with control experiment containing only 2 g/l NaCl in the medium.

Online and offline measurements

Temperature, airflow rate, dissolved oxygen, pH, and cumulative base addition were monitored through data acquisition software supplied by Sartorius (Goettingen, Germany). Samples were withdrawn at regular intervals and analyzed for dry cell weight, glucose, trehalose, lysine, and ammonia. Dry cell weight (DCW) was estimated by using a UV–visible spectrophotometer (Shimadzu/Jasco V-530, Japan). Absorbance was measured at 600 nm. One unit of absorbance was equivalent to 0.28 g/l DCW. Glucose and trehalose were analyzed via a refractive index (RI) detector in HPLC (Hitachi, Merck KgaA, Darmstadt, Germany) using an HP-Aminex-87-H column (Biorad, Hercules, CA, USA) at 65°C with a mobile phase of 5 mM sulfuric acid; flow rate was kept at 0.6 ml/min. Lysine concentration was measured through HPTLC method as reported by Pachuski et al. [20]. Ammonia concentration was measured spectrophotometrically at 410 nm using Nessler's reagent.

Metabolic network structure and computation of elementary modes

The complete set of reactions used for elementary mode analysis is listed elsewhere [7] and comprises reactions involved in glycolysis, the pentose phosphate pathway (PPP), tricarboxylic acid cycle (TCA), anaplerotic reaction converting phosphoenol pyruvate (PEP) into oxaloacetic acid (OaA), and synthesis reactions for glutamate, glutamine, lysine, pyruvate, alanine, and valine. External metabolites considered for this system were glucose, ammonia, oxygen, carbon dioxide, lysine, trehalose, and biomass. These reactions were used to generate elementary modes for the metabolic network of *C. glutamicum* by applying the ScrumPy software package [23]. Stoichiometric coefficients of the external metabolites present in the modes were written in the form of a matrix equation (Eq. 1), where the number of rows was equal to the number

of external metabolites and the number of columns was equal to the number of modes.

Optimization

The set of elementary modes was utilized to obtain the optimal phenotypic space under different conditions. This was achieved by using the 'linprog' module from MATLAB©. The molar mass balances for the metabolites can be written as:

$$S \cdot E = M \quad (1)$$

where M is vector representing the accumulation rates of the external metabolites and S is the matrix, indicating the stoichiometry of the elementary modes. The elements of E $\{e_1, e_2, e_3,\ldots,e_n\}$ represents the vector of unknown fluxes of the elementary modes. The elements of vector E can be evaluated for a given set of measurements of accumulation rates (elements of M). Because of the paucity of measurements, a linear optimization technique can be employed to converge onto a feasible solution. Mathematically, the linear optimization formulation can be represented as Eq. 2:

$$\text{Max } (M_i). \quad (2)$$

Such that $S^*E = M^*$ and $0 \leq e_i \leq \infty$ for all the elementary modes.

M_i is the accumulation rate of a specific metabolite (such as biomass). S^* is the stoichiometric matrix representing the elementary modes and M^* is a known vector of the accumulation rates of extracellular metabolites, wherein the rows of the ith external metabolite are eliminated from S and M, respectively. It should be noted that the above approach of using linear programming to evaluate fluxes is similar to the methodology used in FBA. FBA uses the stoichiometry of the original network for the analysis, whereas we use the stoichiometries of the elementary modes. The unknown fluxes (E) of the elementary modes were obtained by using linear programming. The flux vector E when multiplied with the stoichiometric matrix S gives us the rate vector M, which is further used to map the phenotypic space [7] and to obtain the accumulation rate of an external metabolite through a specific elementary mode. The fluxes of elementary modes were multiplied by the corresponding coefficient in the stoichiometric matrix.

Results

Influence of osmotic stress on growth and metabolite production

Experiments were conducted to determine the growth rate, rate of consumption of substrate (glucose and ammonia), and rate of formation of metabolites (lysine and trehalose) under normal and osmotic stress conditions (25 and 40 g/l of NaCl). Figure 1 shows the concentration profiles for biomass, ammonia, glucose, lysine, and trehalose for the three cases studied and clearly shows an extended lag phase for the uptake of glucose with increase in salt concentration (Fig. 1a). The fermentation time was 32, 40, and 48 h for 0, 25, and 40 g/l of salt concentration, respectively. A similar observation was noted for the uptake of ammonia (Fig. 1b) with residual ammonia of 2 g/l at the end of fermentation. The biomass concentration (Fig. 1c) also demonstrated an extended lag phase with a final DCW of 17, 13, and 11 g/l for 0, 25, and 40 g/l of salt concentration. The specific growth rate for the three cases studied was 0.38, 0.23, and 0.2 h^{-1} for 0, 25, and 40 g/l salt, respectively. The lysine yield also decreased from 0.17 g/g of glucose to 0.12 g/g of glucose for 0 and 40 g/l salt concentration, respectively (Fig. 1d). The lysine synthesis began only after 8, 14, and 20 h of fermentation time for the three cases indicating a delayed accumulation of lysine as a result of the osmotic effect. In the case of trehalose, the yield increased about twofold from 0.016 g/g of glucose to 0.036 g/g of glucose for 0 and 40 g/l salt, respectively. The lag observed for the synthesis of trehalose was similar to that observed for lysine and the synthesis was observed only in the mid log phase of the growth.

In order to evaluate the metabolic fluxes during the growth of *C. glutamicum* on medium containing high salt concentration and compare the same with the control, accumulation rates of substrate and metabolites were determined at different time points (see Fig. S1 in supplementary information at a specific time point). The rates were estimated through derivatives of the fits obtained for the concentration profiles. The details are presented in the supplementary information. These rates were firstly used to evaluate the rates of individual elementary modes and further analyzed to determine the fluxes in the metabolic network.

Quantification of fluxes of elementary modes

The elementary mode analysis yielded 14 modes which represent the central metabolism of *C. glutamicum* (see Table 1) under threonine limitation. The modes capture the conversion of the substrates, glucose, oxygen, and ammonia, to the products, biomass, lysine, and trehalose. Biomass was synthesized in seven modes, while lysine and trehalose were synthesized in nine and five modes, respectively. Out of the seven modes producing biomass, three modes (1–3) synthesized only biomass and among the remaining four either lysine (modes 4, 5) or trehalose (6, 7) were synthesized along with biomass. Maximum theoretical yield of biomass obtained was 115.6/100 mM of

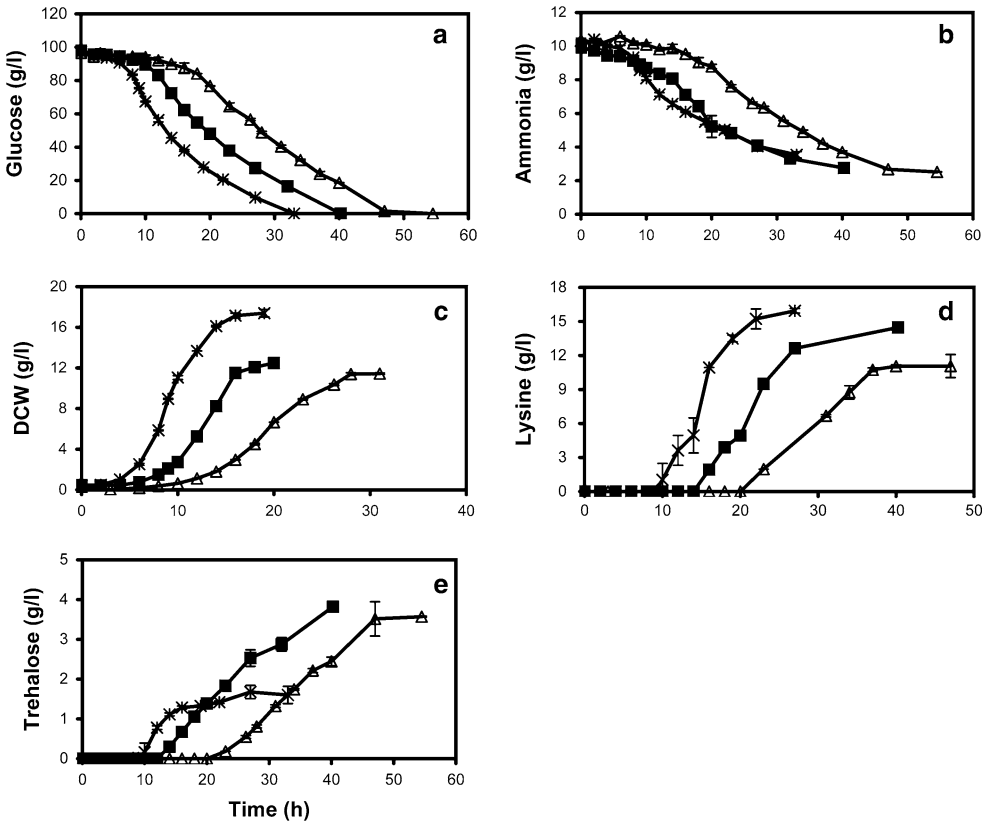

Fig. 1 Comparison of growth experiments on normal medium (0 g/l NaCl) and medium with 25 and 40 g/l NaCl. **a** Glucose concentration, **b** ammonia concentration, **c** biomass as DCW, **d** lysine concentration, and **e** trehalose concentration at various time points. *Asterisks* normal growth; *squares* and *triangles* for experiments with 25 and 40 g/l NaCl in the medium, respectively. All growth experiments were performed with 100 g/l of glucose in the medium

glucose consumed through mode number 1 (Table 1). Lysine was produced in nine modes of which four modes yielded only lysine (modes 8–11), three modes yielded trehalose along with lysine (modes 12–14), and two yielded biomass along with lysine (4, 5). Trehalose was thus not uniquely associated with any of the elementary modes. Maximum theoretical yields of lysine and trehalose were 63.5 and 20/100 mM of glucose consumed through modes 3 and 8, respectively (Table 1). The rank of the matrix formed from the stoichiometry of the metabolites representing the elementary modes was four (matrix S in Eq. 1) implying that the use of four independent accumulation rates as decision variables will uniquely quantify the flux distribution and was also independent of the objective function. The fluxes of the elementary modes were obtained by using the accumulation rates of glucose, lysine, trehalose, and biomass as the decision variables. The fluxes of the elementary modes were a function of the maximization criteria and their mean values along with the standard deviation were plotted at various time points (see Fig. 2).

The fluxes through the 14 elementary modes were used to obtain the contribution of total accumulation rates of various metabolites through the individual elementary modes for normal growth of cells without any salt concentration in the medium (Fig. 2). It is clear from Fig. 2a that most of the glucose uptake occurs through the modes towards biomass (1, 2, and 5) and towards lysine (8–11). Initially, at $t = 6$ h, 90% of the total glucose uptake rate was associated with biomass formation through mode 2, while 8% of the glucose uptake rate yielded lysine (mode 11 only). However at $t = 10$ h, the glucose uptake associated with the modes towards biomass was 60% of the total uptake rate. The remaining 40% was equally distributed between modes yielding biomass and lysine (modes 4 and 5) and modes yielding lysine and trehalose (modes 8 and 14). At $t = 18$ h, 96% of the total glucose uptake rate was towards lysine (modes 8–11) which includes reactions pertaining to glycolysis, TCA, and the anaplerotic reaction representing PEP carboxylase. Thus, the flux values towards various elementary modes clearly demonstrated a transition from biomass-dominating modes to lysine-producing modes representing the effect of limiting threonine in the medium. The flux distribution for the uptake rate of ammonia (Fig. 2b) was similar to that observed for glucose, as glucose and ammonia were associated as substrates for all the modes. Figure 2c shows the flux distribution in various modes for the formation of biomass. During initial exponential phase of growth, most of the biomass was formed through modes yielding only biomass. For example, at $t = 6$ h, 98% of the biomass was formed through mode 2, whereas at $t = 14$ h, the biomass was mainly formed through mode 5 which yield both biomass and lysine. Thus, biomass was mainly accounted for through

Table 1 Elementary modes obtained for the network of *C. glutamicum*

Serial no.	Mode
1	326808 Glucose + 278208 NH_3 + 565083 O_2 → 649566 CO_2 + 378000 Biomass + 1444932 H_2O
2	132444 Glucose + 76544 NH_3 + 410644 O_2 → 433888 CO_2 + 104000 Biomass + 856856 H_2O
3	3166635 Glucose + 1994560 NH_3 + 8993135 O_2 → 9598820 CO_2 + 2710000 Biomass + 19254550 H_2O
4	9492 Glucose + 11352 NH_3 + 14987 O_2 → 20374 CO2 + 2000 Biomass + 40108 H_2O + 4940 Lysine
5	9490 Glucose + 9892 NH_3 + 15619 O_2 → 19698 CO_2 + 6000 Biomass + 40928 H_2O + 2738 Lysine
6	9421984 Glucose + 3756544 NH_3 + 20153144 O_2 → 21293888 CO_2 + 5104000 Biomass + 42051856 H_2O + 1461020 Trehalose
7	8639480 Glucose + 3989120 NH_3 + 17986270 O_2 → 19197640 CO_2 + 5420000 Biomass + 38509100 H_2O + 1153105 Trehalose
8	11 Glucose + 14 NH_3 + 17 O_2 → 24 CO_2 + 46 H_2O + 7 Lysine
9	36 Glucose + 44 NH_3 + 62 O_2 → 84 CO_2 + 160 H_2O + 22 Lysine
10	63 Glucose + 72 NH_3 + 126 O_2 → 162 CO_2 + 306 H_2O + 36 Lysine
11	3 Glucose + 2 NH_3 + 11 O_2 → 12 CO_2 + 22 H_2O + 1 Lysine
12	112 Glucose + 112 NH_3 + 196 O_2 → 252 CO_2 + 476 H_2O + 7 Trehalose + 56 Lysine
13	38 Glucose + 44 NH_3 + 62 O_2 → 84 CO_2 + 160 H_2O + 1 Trehalose + 22 Lysine
14	5 Glucose + 2 NH_3 + 11 O_2 → 12 CO_2 + 22 H_2O + 1 Trehalose + 1 Lysine

Serial number identifies a specific elementary mode used in the text

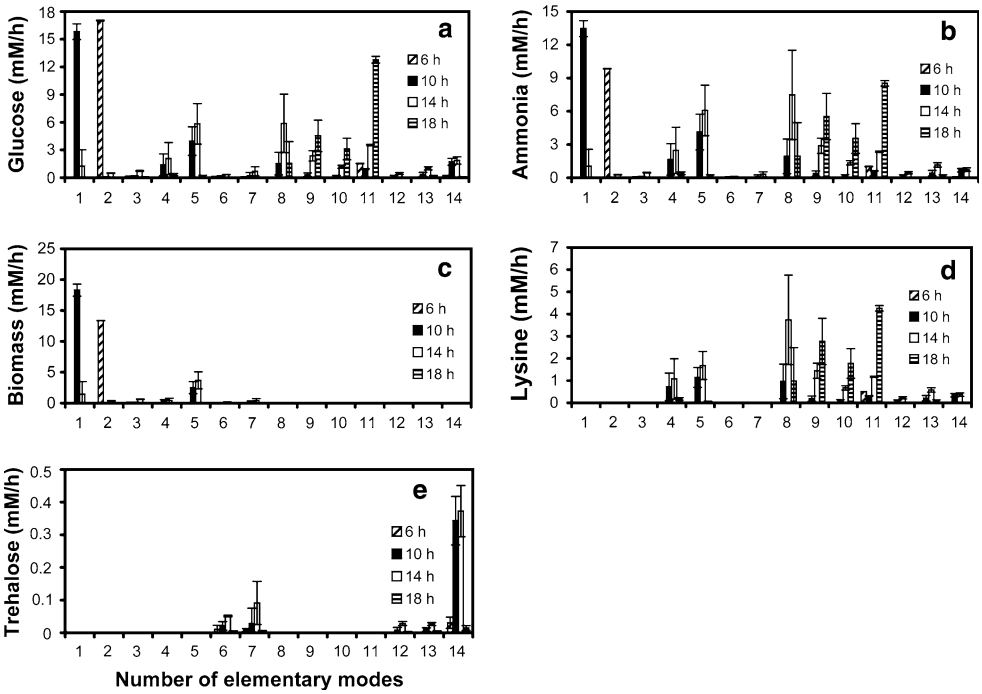

Fig. 2 Histogram of flux values through the 14 elementary modes for various metabolites under normal growth conditions with 100 g/l glucose in the medium. The fluxes were computed by linear programming using maximization of ammonia, O_2, and CO_2 as objective function and average is shown as histogram with standard deviation. Uptake rate of glucose and production rates of lysine, trehalose, and biomass were used as decision variables. **a** Glucose consumption rate, **b** ammonia consumption rate, **c** biomass formation rate, **d** lysine formation rate, and **e** trehalose formation rate. The fluxes are shown for time points $t = 6$, 10, 14, and 18 h

three modes with a shift from modes yielding only biomass (modes 1 and 2) to modes yielding both biomass and lysine (mode '5').

An opposite trend was observed for lysine synthesis (Fig. 2d), wherein the dominant lysine-yielding modes were active at $t = 14$ and 18 h (modes 8–11). Trehalose was mainly produced between 10 and 14 h using the elementary mode number '14'. Further, modes associated with both biomass and trehalose were also active accounting for about 25% of the total flux towards trehalose. Although these modes contributed significantly towards trehalose formation, their contribution towards biomass was meager (about 8%).

Under osmotic stress conditions (induced by 40 g/l NaCl), the numbers of active modes were less as compared with the normal growth conditions (Fig. 3). It is clear from Fig. 3a that most of the glucose uptake occurs through the modes towards biomass (2, 3, and 5) and towards lysine (11 and 14). At $t = 16$ h, 75% of the total glucose uptake rate was associated with biomass formation mainly through

mode 2, while 15% of the glucose uptake rate yielded lysine (mode 11 only). However, at 18 and 20 h, mode 3 also became prominent. At $t = 18$ h the glucose uptake associated with the modes towards biomass was approximately 73%, while it was 67% at $t = 20$ h. The remaining glucose was distributed among modes yielding biomass and lysine (modes 4 and 5) and modes yielding lysine and trehalose (modes 11 and 14) at $t = 18$ and 20 h. At $t = 22$ h, modes 1–3 and 11 were significantly active. Together, purely biomass-forming modes (mode 1–3) carried 55% of the total glucose consumed, while 27% of the glucose uptake rate was associated with mode 11 forming lysine. Thus, it is clear from the flux values towards various elementary modes that flux carried by purely biomass-forming modes gradually decreased with time, whereas it increased with time for lysine-forming modes. Under stress the flux distribution through various modes for the uptake rate of ammonia (Fig. 3b) was similar to that observed for glucose. Figure 3c shows the flux distribution in various modes for the formation of biomass. Approximately 90% of the biomass was produced through only biomass-forming modes (modes 1–3) at all the times studied. The remaining 10% was mainly contributed through mode 5 (forming biomass and lysine) at $t = 18$ and 20 h and by mode 6 (forming biomass and trehalose) at $t = 22$ h. Under stress conditions lysine was mainly produced through modes 4, 5, and 11, while the rest of the lysine-producing modes (modes 8–10) contributed not more than 15% towards lysine formation (Fig. 3d). Under osmotic stress conditions as well most of the trehalose was produced through modes 6, 7, and 14, but the flux carried by modes producing biomass and trehalose simultaneously (modes 6 and 7) was higher under osmotic stress conditions as compared with the normal growth conditions.

Thus, in essence, the analysis revealed the dominance of various modes with the progression of fermentation for uptake or formation of a particular metabolite. Also under osmotic stress the metabolism behaved rigidly, which was reflected through lesser numbers of modes being active under this condition as compared with normal growth. The higher rigidity is further reflected by the lower value of standard deviation under osmotic stress conditions.

Metabolic flux distribution

Flux distribution for the metabolic network of *C. glutamicum* was obtained for the three conditions namely medium with 0, 25, and 40 g/l salt in the growth medium (numbers from top to bottom, respectively in Fig. 4). The flux distribution shown in Fig. 4 was obtained at the mid log phase for the three cases representing the fluxes at times 10, 14, and 20 h, respectively. The fluxes were normalized with respect to the glucose uptake rates observed at the specific time. Under normal conditions, 60% of the flux from the glucose uptake was routed through the pentose phosphate and the remaining into the glycolytic (35%) and trehalose synthesis (1.5%). The flux towards biomass and lysine formation was 80 and 15, respectively. Further, the oxygen uptake rate of 181 resulted in ATP dissipation of 524 with respect to glucose uptake of 100 mM/h. It can be noted that

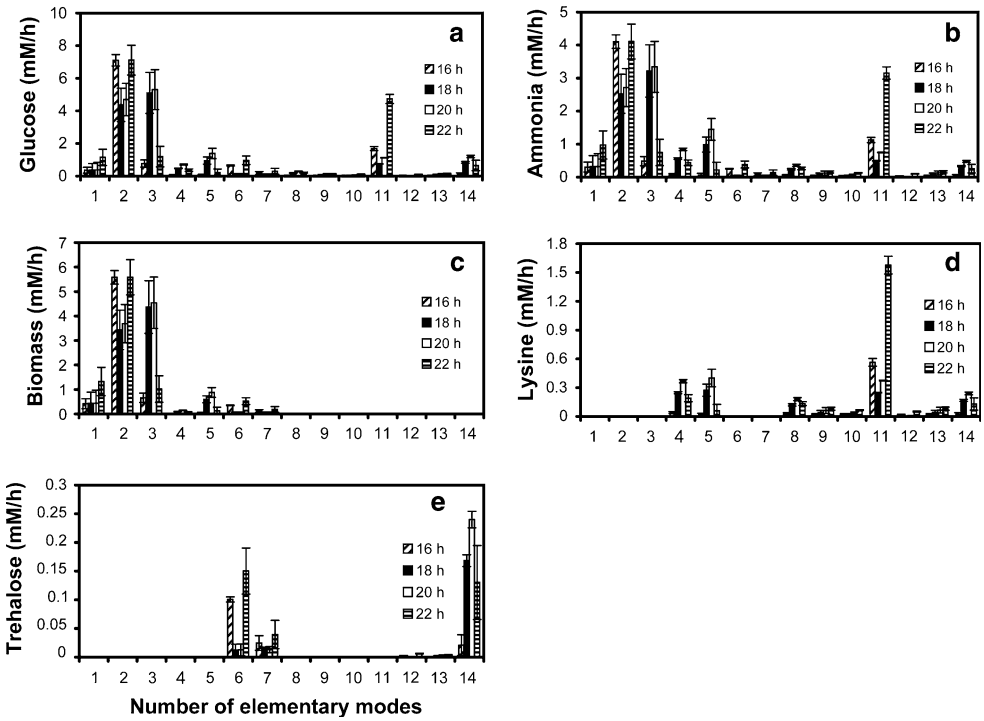

Fig. 3 Histogram of flux values through the 14 elementary modes for various metabolites under osmotic stress with 100 g/l glucose and 40 g/l NaCl in the medium. The fluxes were computed by linear programming using maximization of ammonia, O_2, and CO_2 as objective function and average is shown as histogram with standard deviation. Uptake rate of glucose and production rates of lysine, trehalose, and biomass were used as decision variables. **a** Glucose consumption rate, **b** ammonia consumption rate, **c** biomass formation rate, **d** lysine formation rate, and **e** trehalose formation rate. The fluxes are shown for time points $t = 16$, 18, 20, and 22 h

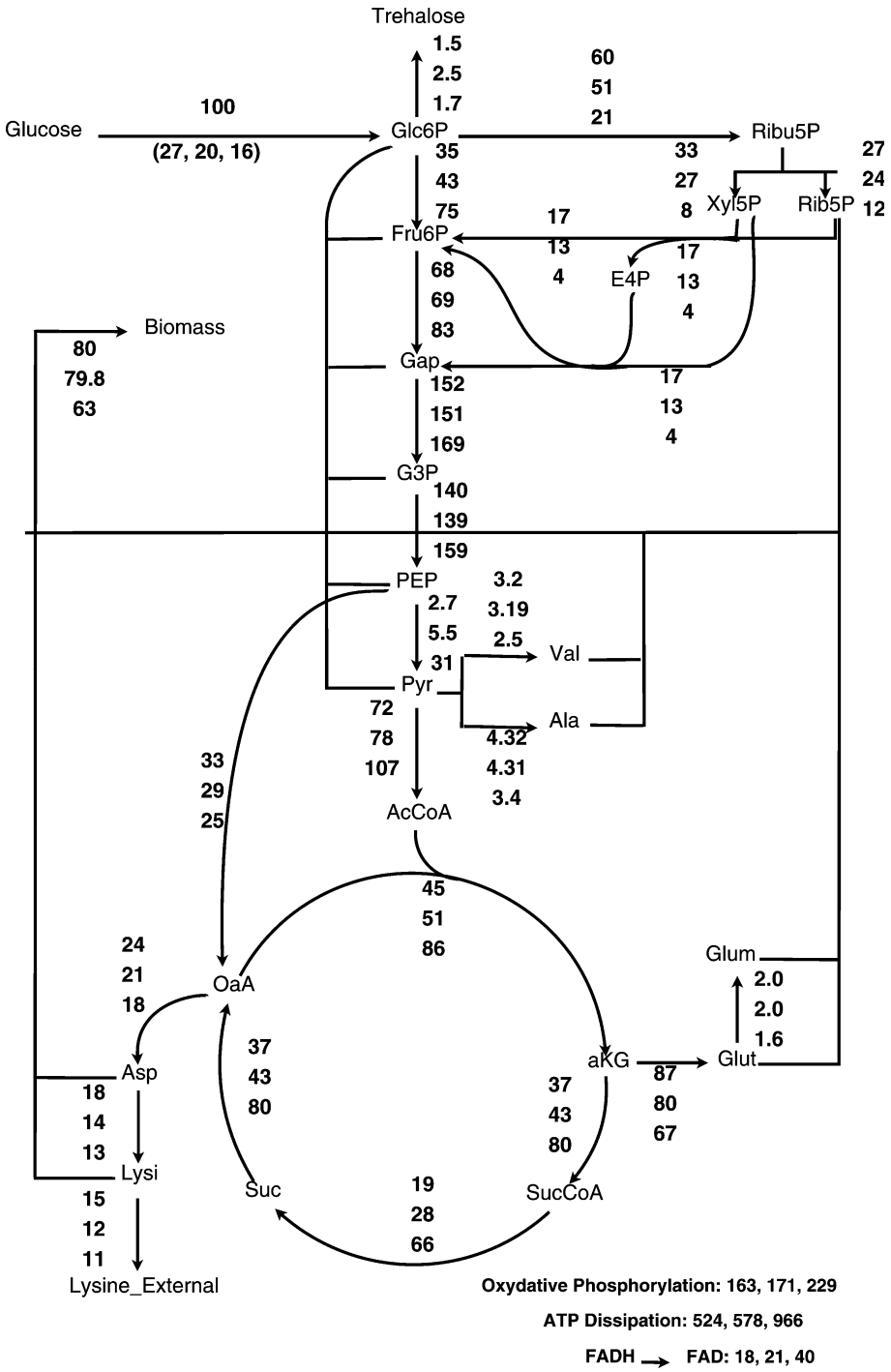

Fig. 4 Flux distribution map for growth of *C. glutamicum* on medium containing 0, 25, and 40 g/l NaCl and having 100 g/l initial glucose concentration. The flux distributions were obtained at mid log phase growth at $t = 10$, 14, and 20 h for the growth on 0, 25, and 40 g/l NaCl, respectively. Numerical values from *top* to *bottom* for each flux value indicate for the condition of growth with no salt, 25, and 40 g/l NaCl, respectively. The fluxes were expressed in mM/h and normalized with respect to the glucose uptake rate. The absolute glucose uptake rates for growth on medium with 0, 25, and 40 g/l NaCl were 27, 20, and 16 mM/h, respectively (also shown in parenthesis)

under osmotic shock, the flux towards the pentose phosphate pathway was reduced by one-third for the case with 40 g/l salt relative to the normal concentration. Further, the flux through the TCA cycle was doubled resulting in increased oxygen uptake rate of about 270. The ATP dissipation also doubled relative to the normal cell growth. Under osmotic shock, the fluxes towards biomass and lysine reduced by 25 and 40%, respectively. The analysis indicated that most of the carbon from the glucose was released as carbon dioxide through the TCA cycle. Further, the decreased flux towards lysine was correlated with a decreased flux in the PEP carboxylase reaction.

The flux distribution in the network is typically evaluated at a specific time point at which the accumulation rate is experimentally determined. The flux distributions at various time points during the fermentation were also determined (results not shown). Under normal growth conditions, it was observed that initially the flux through

the TCA cycle was high. However, as the rate of production of biomass picked up, the flux through TCA cycle reduced. The flux through the pentose phosphate pathway increased with time to support biomass and lysine synthesis; later with decline in the biomass synthesis rate, flux through the PPP pathway also declined. Further, anaplerotic flux of PEP to OaA through PEP carboxylase increased with increase in lysine production rate. Under such a condition, the flux through PEP carboxylase was dominant as compared with the conversion of PEP to pyruvate. In the case of growth under osmotic stress, a similar result was observed, but with an increased flux through TCA and a reduced flux through the anaplerotic reaction as compared with that observed for normal growth.

Principal node analysis

The metabolic network of *C. glutamicum* has four principal nodes, namely glucose-6-phosphate (Glc6p), phosphoenol pyruvate (PEP), pyruvate (Pyr), and oxaloacetic acid (OaA). Because a nodal metabolite acts as a substrate for multiple reactions, split ratio can be evaluated to determine the ratio of fluxes in the individual output fluxes with respect to the net input flux. In the G1c6p node (see Fig. 4), 60% of the net glucose uptake flux was routed through the pentose pathway, while remaining 35 and 1.5% was distributed between glycolytic pathway and trehalose synthesis, respectively. Upon osmotic shock, the fluxes through the pentose phosphate pathway (PPP) branch reduced by about 70% while the flux through the glycolytic pathway increased by approximately twofold. Thus, at the G1c6p node, osmolality has a key effect of reorienting the fluxes through the PEP and glycolytic pathway to balance the reduced requirement of NADPH. The split ratio at PEP node is shown in Fig. 5a. PEP is used as a substrate in the PTS for uptake of glucose and in the glycolytic pathway to form pyruvate. PEP is also connected to OaA through the PEP carboxylase reaction. Most of the PEP pool was used up in the phosphotransferase system (PTS) and there was a reduction of about 10% in the split ratio through PTS as a result of increased osmolality. Because of reduced lysine formation under osmotic stress conditions, the split ratio reduced in the anaplerotic reaction by 30%. The flux through the glycolytic path increased by tenfold to compensate for the reduction in the other two branches. At the pyruvate node (see Fig. 5b), the flux through the TCA cycle increased by 20% as a result of increased osmolality, and decreased by 40 and 30% in the branches towards lysine and amino acid synthesis, respectively. At the OaA node, the net OaA synthesized was due to the anapleroic flux of PEP carboxylase and it branches out for the synthesis of glutamate and aspartate. The overall distribution

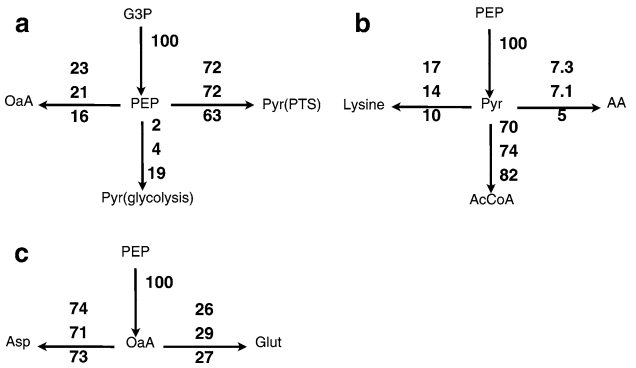

Fig. 5 Split ratios at the principal nodes of **a** phosphoenol pyruvate (*PEP*), **b** pyruvate (*Pyr*), and **c** oxaloacetic acid (*OaA*) normalized with respect to the formation of the individual metabolites. Numerical values from *top* to *bottom* indicate the flux for the experimental condition with no salt, 25, and 40 g/l NaCl, respectively, for mid log phase of growth. In **a**, *Pyr* (*PTS*) and *Pyr* (*glycolysis*) indicate the formation of pyruvate through phosphotransferase system (*PTS*) and through glycolysis, respectively. Synthesis of alanine and valine are lumped together and are represented as *AA* in panel **b**

of fluxes was not affected by osmolality for this node. To summarize the nodal analysis, fluxes were reoriented at the G1c6p, PEP, and the pyruvate nodes as a result of increased osmolality.

Analysis of optimal phenotypic space

The phenotypic space of *C. glutamicum* can be obtained by evaluating the metabolic capability by solving Eq. 2 and by invoking constraints of uptake rates of glucose, ammonia, and oxygen. It can be noted that four accumulation rates yield a unique solution, although by constraining the elementary modes using only three uptake rates, phenotypic space of the organism for various objective functions can be obtained. Optimal phenotypic spaces thus obtained for maximization of biomass, lysine, and trehalose separately are presented in Fig. 6. The maximum flux towards biomass was 115.6 mM/h with corresponding ammonia and oxygen uptake rates of 85 and 173 mM/h, respectively (Fig. 6a). The bounds for the ammonia and oxygen uptake rates for maximizing biomass were 40–127 and 155–366 mM/h, respectively. The phenotypic space for maximizing lysine production is shown in Fig. 6b. The maximum yield for lysine was 63.5/100 mM of glucose with ammonia and oxygen uptake rates to be 127 and 155 mM/h, respectively. The bounds for the ammonia and oxygen uptake rates were the same as that obtained for the phenotypic space for maximizing biomass. The maximum trehalose yield was found to be 19.9/100 mM of glucose with corresponding ammonia and oxygen uptake rates of 40 and 220 mM/h, respectively. The optimal phenotypic space for various objective functions thus provides the metabolic capability of the organism.

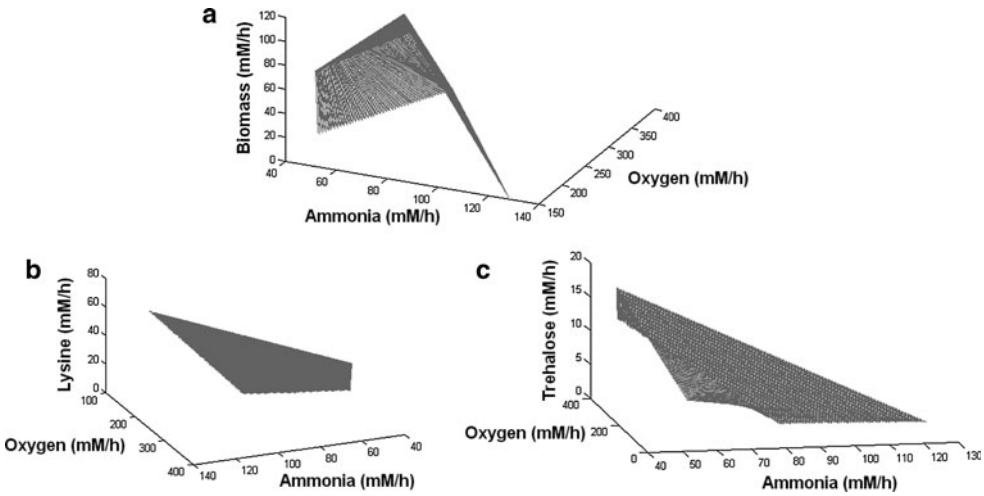

Fig. 6 Optimal phenotypic spaces for the maximization of **a** biomass, **b** lysine, and **c** trehalose as an objective function. The uptake rate of glucose was fixed at 100 mM/h and biomass, lysine, and trehalose synthesis rates were plotted at various ammonia and oxygen consumption rates. The maximum theoretical yields for biomass, lysine, and trehalose were 115.6, 63.5, and 19.9 mM/100 mM of glucose, respectively. All three phenotypic spaces yield similar bounds on oxygen and ammonia uptake rates of 155–366 and 40–127 mM/h, respectively

The optimal feasible accumulation rates for the objective function of biomass, lysine, and trehalose optimization were compared at different time points with that obtained experimentally (see Fig. 7). Figure 7a compares experimentally measured biomass rates with the optimal biomass rates obtained from maximization of biomass. It was observed that the rate of biomass formation at $t = 6$ h obtained experimentally was equal to that obtained by using the maximization of biomass, indicating that the organism optimizes growth at this hour. This also implies that the experimental value lies on the optimal phenotypic space as shown in Fig. 6a. Although optimal, the value at $t = 6$ h was only 60% of the maximum theoretical feasible value of 115 mM/h. This is due to the fact that the ammonia and oxygen uptake rates relative to glucose uptake rate were limiting. However, the biomass formation rates deviate from the optimal feasible values as time proceeds, with the difference being largest at $t = 12$ h, with a decrease of 1.5-fold relative to the optimal value. The experimental value was relatively closer to the optimal feasible formation rates at the end of fermentation, albeit the rates themselves were low as the organism reaches the stationary phase.

Figure 7b shows the comparison between the optimal feasible accumulation rates for lysine using the objective function of maximizing lysine formation rates, with that obtained through experiments. It is clear from the figure that the lysine formation rates were suboptimal up to 16 h, with the maximum deviation at the beginning of cell growth, with a tenfold decrease in the experimental value relative to the optimal value at $t = 6$ h. Beyond 16 h, the experimental value lies in the feasible optimal space of lysine maximization. The maximum rate of lysine formation of about 48 mM/h was observed at $t = 16$ h which was 75% of the maximum theoretical value of 63.5 mM/h. A similar behavior was observed for the trehalose formation rates, wherein the maximum deviation from the feasible optimal value was observed at $t = 6$ h with a 26-fold decrease in the experimental value relative to the optimal value observed. A maximum trehalose formation rate of 2.3 mM/h during the period $t = 12$–14 h was observed, which was only 12% of the maximum theoretical feasible rate.

The optimal feasible accumulation rates for the various objective functions under 40 g/l of salt stress were also compared with experimental values. Analysis was done for the data between 14 and 22 h, which covers the exponential phase of growth of the organism, because the organism was in the lag phase until $t = 12$ h. Figure 7d shows a comparison of the optimal and experimental values for the biomass formation rate. Under stress, the experimental biomass formation rate was always lower than the optimal feasible biomass formation rates, with a maximum of 1.4-fold decrease of the experimental value relative to the optimal value at $t = 22$ h. The observed biomass formation rates were relatively invariant from $t = 14$ to 20 h with an average rate of 65 mM/h. This rate was 43% less than the maximum theoretical biomass formation rate of 115 mM/h. Figure 7e shows a comparison between the experimental lysine formation rates with the optimal feasible rates of lysine formation. A linear increase in the rate was observed from 5 to 14 mM/h between $t = 14$ h and $t = 22$ h, thus showing gradual reduction in the difference between experimental and optimal feasible values with time. Maximum difference between experimental and optimal feasible rates was observed at $t = 14$ h, where the experimental value was sixfold less than that of the optimal value. Further, the lysine formation rate was only 42% of the optimal feasible value at $t = 22$ h. A similar observation was made for the trehalose formation, wherein the optimal feasible rate was invariant in time at approximately 7.4 mM/h and the experimentally observed values were in the range of 1–2 mM/h during $t = 14$–22 h. These values were comparable to the values observed under normal

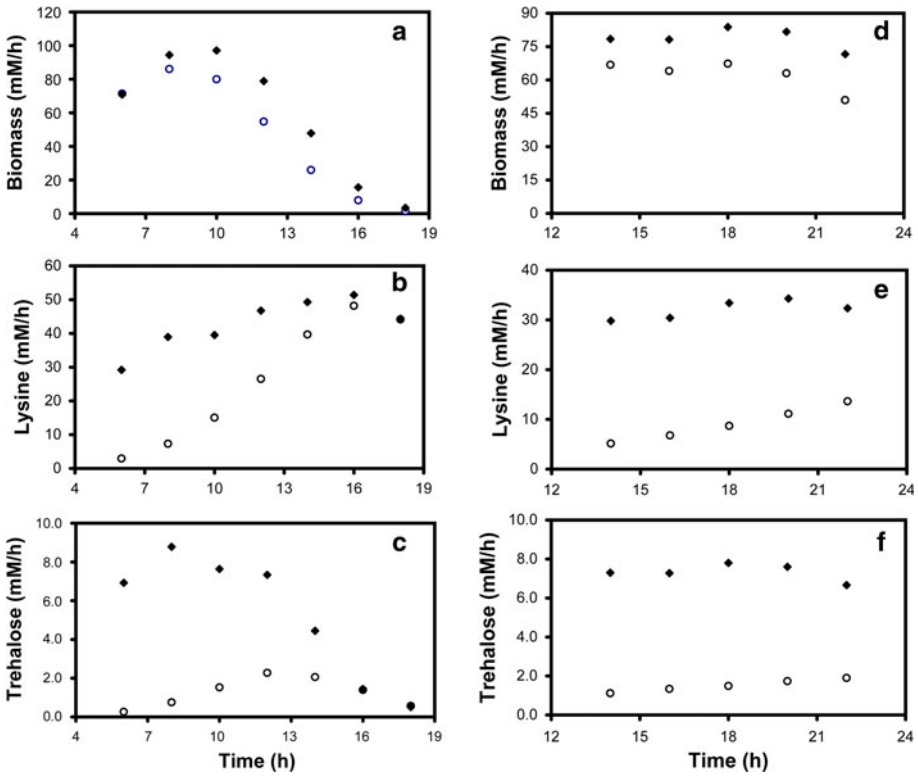

Fig. 7 Comparison of predicted optimal rates (*diamonds*) with that obtained from experiments (*circles*) at various fermentation time points for the three different maximization criteria, namely biomass, lysine, and trehalose for growth (**a**–**c**) under normal conditions and (**d**–**f**) under osmotic stress (40 g/l NaCl), respectively

conditions. The comparison under the condition of shock indicates that during fermentation none of the accumulation rates lie on the optimal feasible values. A comparison of observed accumulation rates with the values for the optimal feasible rates at 25 g/l of salt also indicated that the observed rates do not lie on the optimal feasible space (see Fig. S2 in the supplementary information); however, the deviation from the optimal was not as severe as that for 40 g/l of salt.

Discussion

Microorganisms alter their metabolic status during stress conditions. Stress conditions also induce an adaptive phase during which the cell suspends its growth. To evaluate the effect of increased osmolality on the metabolic status of *C. glutamicum*, elementary mode analysis was applied to the metabolic network. Growth experiments were performed with and without osmotic stress to determine the accumulation rates of various metabolites, which were used to evaluate the fluxes in the elementary modes and in the metabolic network. Growth experiments demonstrated an extended lag phase under the influence of higher osmolality. The uptake rates of glucose and ammonia were also reduced, thereby increasing the fermentation times. While biomass and lysine yields were reduced, the yield of trehalose, a storage compound, increased as a result of increased osmolality. Trehalose is known to be a compatible solute under stress by protecting proteins and cellular membrane from denaturation [1, 6]. In the strain of *C. glutamicum* studied, accumulation of amino acids such as proline and glutamate was not observed; however, previous studies reported that amino acids other than lysine accumulate under stress conditions [8, 9, 25].

Elementary mode analysis yielded 14 modes that represent the metabolic network of *C. glutamicum* under both conditions of normal and stressed growth. The substrates were glucose, ammonia, and oxygen, while products were lysine, trehalose, and biomass. The elementary modes were further used to evaluate the fluxes through the metabolic network using optimization under the stoichiometric constraint represented by the matrix equation (Eq. 1). The flux distribution provided insights into the relative importance of various pathways under osmotic stress conditions. Under osmotic stress, higher flux was observed through energy-generating pathways, namely glycolysis and TCA cycle and oxidative phosphorylation yielding excess ATP. The increased flux through ATP dissipation reaction demonstrates the increased energy demand under osmotic stress conditions as maintenance was high compared with the normal growth conditions. The flux through the pentose phosphate pathway reduced with increasing osmolality as a result of reduced demand for NADPH, which was required for anabolic reactions such as synthesis of amino acids and biomass. However, the flux towards trehalose increased as

a result of osmotic stress, and trehalose is known to stabilize the intracellular proteins [3, 6]. The analysis also indicated that a considerable amount of carbon, available as a result of reduced biomass and lysine formation, was released as carbon dioxide that is generated through TCA cycle for ATP formation.

Nodal analysis showed that Glc6P, PEP, and pyruvate nodes were capable of adapting to increasing osmolality. This was evident from the reduced flux partitioning through PPP branch at the Glc6P node. The split ratio reduced because of the reduction in the amount of metabolites (lysine, biomass, and other amino acids) produced. A similar observation applied to the other two nodes, indicating flexibility at these nodes for flux partitioning. On the other hand, OaA node exhibited relative inflexibility as evident from no substantial change in the flux partitioning. The last observation is in agreement with the results reported by Varela et al. [32], who reported that OaA shows rigidity up to 1,000 mosmol/kg [32, 33].

We also characterized the optimal phenotypic space using linear optimization. Here the uptake rates of substrates were utilized as constraints and maximization of a metabolite production rate was given as an objective function. Such an analysis allows the determination of the optimal/suboptimal behavior of the organism under a given set of conditions. Specifically, if the point representing the experimental observation lies below the optimal solution space, it can be inferred that although the solution is feasible, the organism is suboptimal for the synthesis of the particular metabolite. Experimental data points for the three conditions plotted with respect to time and compared with the optimal biomass, lysine, and trehalose rates for maximization of biomass, lysine, and trehalose as an objective function, respectively, indicated that for normal growth conditions the experimental point noted at $t = 6$ h was in the optimal solution space for maximization of biomass, and the experimental points noted at $t = 16$ and 18 h were in the space obtained for trehalose maximization. However, the average deviation across fermentation time was only 1.6-fold less than that obtained under optimal conditions for biomass formation. This analysis thus demonstrated that under normal growth conditions, *C. glutamicum* tends to maximize biomass production [7]; later as time progresses and fermentation conditions become less conducive for growth, it shifts to optimize lysine (in threonine-limiting conditions) and trehalose production (a storage compound). For the growth condition under osmotic stress, none of the experimental points were in the optimal space and the average deviation across fermentation was 1.3-fold less than the predicted optimal values. Thus, the cells do not maximize growth under osmotic stress conditions because a fraction of the resources consumed were utilized for the adaptation process. Although *C. glutamicum* increased trehalose synthesis under stress, the flux towards its synthesis was not optimal. Thus, under stress, the cells tend to use the carbon from glucose to route it through TCA cycle for increased synthesis of ATP by releasing the carbon in the form of carbon dioxide.

In summary, *C. glutamicum* readjusts its metabolic state in order to adapt to osmotic stress. Firstly, the organism extends its lag phase, during which time the cell devision is halted and the cells adapt to the stress. The phenotypic state of the cells is altered with a reduced glucose and ammonia uptake rates with lower biomass and lysine formation. The flux towards trehalose is increased to counter the stress and to stabilize the intracellular proteins. The flux through the TCA cycle was increased to balance the increased demands for ATP. The split ratio at various nodes indicated that the nodes in the glycolytic pathway were flexible to readjust the fluxes necessary as a result of the stress. Further, fluxes through the elementary modes demonstrated that fewer modes are used under stress compared with that observed under normal growth. The optimal phenotypic space was used to determine the extent of the capability of the organism and the actual performance of the organism. As expected, it was observed that the cells were farther away from optimality under stress as compared with normal growth. Analysis presented here incorporates the central carbon and nitrogen metabolism in *C. glutamicum*. It is expected that the central metabolism would not be different at least in various strains of *C. glutamicum*. In this respect, the results will be indicative for various strains of *C. glutamicum*. Further, the phenomenon of suboptimal behavior under osmotic stress conditions may be valid for different strains of *C. glutamicum* that accumulate lysine. Thus, the elementary mode analysis is a powerful tool to obtain functional insights into the performance of metabolic networks and to quantify phenotypic behavior of an organism.

References

1. Arakawa T, Timasheff SN (1985) The stabilization of proteins by osmolytes. Biophys J 47:411–414
2. Benjamin F, Christian T, Christian R, Jörn K, Ansgar P, Dirk Andreas W (2010) Adaptation of *Corynebacterium glutamicum* to salt-stress conditions. Proteomics 10:445–457
3. Bolen DW, Rose GD (2008) Structure and energetics of the hydrogen-bonded backbone in protein folding. Annu Rev Biochem 77:339–362
4. Csonka LN (1989) Physiological and genetic responses of bacteria to osmotic-stress. Microbiol Rev 53:121–147
5. Csonka LN, Hanson AD (1991) Prokaryotic osmoregulation—genetics and physiology. Annu Rev Microbiol 45:569–606
6. Elbein AD, Pan YT, Pastuszak I, Carroll D (2003) New insights on trehalose: a multifunctional molecule. Glycobiology 13:17R–27R

7. Gayen K, Venkatesh KV (2006) Analysis of optimal phenotypic space using elementary modes as applied to *Corynebacterium glutamicum*. BMC Bioinformatics 7:445
8. Guillouet S, Engasser JM (1995) Growth of *Corynebacterium glutamicum* in glucose-limited continuous cultures under high osmotic pressure. Influence of growth rate on the intracellular accumulation of proline, glutamate and trehalose. Appl Microbiol Biotechnol 44:496–500
9. Guillouet S, Engasser JM (1995) Sodium and proline accumulation in *Corynebacterium glutamicum* as a response to an osmotic saline upshock. Appl Microbiol Biotechnol 43:315–320
10. Heermann R, Jung K (2004) Structural features and mechanisms for sensing high osmolarity in microorganisms. Curr Opin Microbiol 7:168–174
11. Kempf B, Bremer E (1998) Uptake and synthesis of compatible solutes as microbial stress responses to high-osmolality environments. Arch Microbiol 170:319–330
12. Knowles CJ, Smith L (1971) Effect of osmotic pressure of medium on volume of intact cells of *Azotobacter vinelandii* and on rate of respiration. Biochim Biophys Acta 234:144–152
13. Kramer R (2009) Osmosensing and osmosignaling in *Corynebacterium glutamicum*. Amino Acids 37:487–497
14. Mitchell P, Moyle J (1956) Osmotic function and structure in bacteria. In bacterial anatomy. Symp SOC gen Microbiol 6:150
15. Möker N, Brocker M, Schaffer S, Krämer R, Morbach S, Bott M (2004) Deletion of the genes encoding the MtrA–MtrB two-component system of *Corynebacterium glutamicum* has a strong influence on cell morphology, antibiotics susceptibility and expression of genes involved in osmoprotection. Mol Microbiol 54:420–438
16. Moker N, Kramer J, Unden G, Kramer R, Morbach S (2007) In vitro analysis of the two-component system MtrB–MtrA from *Corynebacterium glutamicum*. J Bacteriol 189:3645–3649
17. Moker N, Reihlen P, Kramer R, Morbach S (2007) Osmosensing properties of the histidine protein kinase MtrB from *Corynebacterium glutamicum*. J Biol Chem 282:27666–27677
18. Morbach S, Kramer R (2002) Body shaping under water stress: osmosensing and osmoregulation of solute transport in bacteria. Chembiochem 3:385–397
19. Morbach S, Kramer R (2003) Impact of transport processes in the osmotic response of *Corynebacterium glutamicum*. J Biotechnol 104:69–75
20. Pachuski J, Fried B, Sherma J (2002) HPTLC analysis of amino acids in *Biomphalaria glabrata* infected with *Schistosoma mansoni*. J Liq Chromatogr Relat Technol 25:2345–2349
21. Papin JA, Stelling J, Price ND, Klamt S, Schuster S, Palsson BO (2004) Comparison of network-based pathway analysis methods. Trends Biotechnol 22:400–405
22. Poolman B, Glaasker E (1998) Regulation of compatible solute accumulation in bacteria. Mol Microbiol 29:397–407
23. Poolman MG (2006) ScrumPy: metabolic modelling with Python. IEE Proc Syst Biol 153:375–378
24. Primm TP, Andersen SJ, Mizrahi V, Avarbock D, Rubin H, Barry CE (2000) The stringent response of *Mycobacterium tuberculosis* is required for long-term survival. J Bacteriol 182:4889–4898
25. Ronsch H, Kramer R, Morbach S (2003) Impact of osmotic stress on volume regulation, cytoplasmic solute composition and lysine production in Corynebacterium glutamicum MH20–22B. J Biotechnol 104:87–97
26. Schuster S, Dandekar T, Fell DA (1999) Detection of elementary flux modes in biochemical networks: a promising tool for pathway analysis and metabolic engineering. Trends Biotechnol 17:53–60
27. Skjerdal OT, Sletta H, Flenstad SG, Josefsen KD, Levine DW, Ellingsen TE (1995) Changes in cell volume, growth and respiration rate in response to hyperosmotic stress of NaCl, sucrose and glutamic acid in *Brevibacterium lactofermentum* and *Corynebacterium glutamicum*. Appl Microbiol Biotechnol 43:1099–1106
28. Skjerdal OT, Sletta H, Flenstad SG, Josefsen KD, Levine DW, Ellingsen TE (1996) Changes in intracellular composition in response to hyperosmotic stress of NaCl, sucrose or glutamic acid in *Brevibacterium lactofermentum* and *Corynebacterium glutamicum*. Appl Microbiol Biotechnol 44:635–642
29. Stackebrandt E, Rainey FA, Ward-Rainey NL (1997) Proposal for a new hierarchic classification system, Actinobacteria classis nov. Int J Syst Bacteriol 47:479–491
30. Trinh C, Wlaschin A, Srienc F (2009) Elementary mode analysis: a useful metabolic pathway analysis tool for characterizing cellular metabolism. Appl Microbiol Biotechnol 81:813–826
31. Vallino JJ, Stephanopoulos G (1993) Metabolic flux distributions in *Corynebacterium glutamicum* during growth and lysine overproduction. Biotechnol Bioeng 41:633–646
32. Varela C, Agosin E, Baez M, Klapa M, Stephanopoulos G (2003) Metabolic flux redistribution in *Corynebacterium glutamicum* in response to osmotic stress. Appl Microbiol Biotechnol 60:547–555
33. Varela CA, Baez ME, Agosin E (2004) Osmotic stress response: quantification of cell maintenance and metabolic fluxes in a lysine-overproducing strain of *Corynebactetium glutamicum*. Appl Environ Microbiol 70:4222–4229
34. Wolf A, Kramer R, Morbach S (2003) Three pathways for trehalose metabolism in *Corynebacterium glutamicum* ATCC13032 and their significance in response to osmotic stress. Mol Microbiol 49:1119–1134